Mon. Not. R. Astron. Soc. **335,** 1049–1053 (2002)

Edge-on boxy profiles in non-barred disc galaxies

P. A. Patsis,[1⋆] E. Athanassoula,[2] P. Grosbøl[3] and Ch. Skokos[1,4]

[1]*Research Center of Astronomy, Academy of Athens, Anagnostopoulou 14, GR-10673 Athens, Greece*
[2]*Observatoire de Marseille, 2 Place Le Verrier, F-13248 Marseille Cedex 4, France*
[3]*ESO, Karl Schwarzschild Strasse 2, D-85748 Garching bei München, Germany*
[4]*Division of Applied Analysis, Department of Mathematics and Center for Research and Application of Nonlinear Systems (CRANS), University of Patras, GR-26500 Patras, Greece*

Accepted 2002 May 14. Received 2002 April 11; in original form 2002 January 30

ABSTRACT

Boxy edge-on profiles can be accounted for not only in models of barred galaxies, but also in models of normal (non-barred) galaxies. Thus the presence of a bar is not a sine qua non condition for the appearance of this feature, as often assumed. We show that a 'boxy' or a 'peanut' structure in the central parts of a model is due to the presence of vertical resonances at which stable families of periodic orbits bifurcate from the planar x1 family. The orbits of these families reach in their projections on the equatorial plane a maximum distance from the centre, beyond which they increase their mean radii by increasing only their deviations from the equatorial plane. The resulting orbital profiles are 'stair-type' and constitute the backbone for the observed boxy structures in edge-on views of *N*-body models and, we believe, in edge-on views of disc galaxies. Since the existence of vertical resonances is independent of barred or spiral perturbations in the disc, 'boxy' profiles may appear also in almost axisymmetric cases.

Key words: galaxies: evolution – galaxies: kinematics and dynamics – galaxies: structure.

1 INTRODUCTION

A significant number of edge-on disc galaxies display in their inner regions a 'boxy' or 'peanut'-shaped (hereafter b/p) structure. It is believed (Lütticke, Dettmar & Pohlen 2000) that more than 45 per cent of disc galaxies have this kind of edge-on profile. Typical examples are NGC 2424, NGC 6771, NGC 5746, IC 4767, Hickson 87a and the Milky Way. Several authors (Combes & Sanders 1981; Pfenniger 1984, 1985; Combes et al. 1990; Pfenniger & Friedli 1991; Raha et al. 1991; Kuijken & Merrifield 1995; Bureau & Freeman 1999) have related these profiles to the presence of a strong bar. The tangential force in these bars is typically of the order of 25 per cent of the axisymmetric one (Combes & Sanders 1981).

Patsis & Grosbøl (1996) have shown that b/p orbital profiles appear also in cases with a spiral instead of a bar perturbation. Recently Athanassoula (in preparation) made a large number of *N*-body simulations to follow the formation and evolution of bars in isolated bar-unstable discs. Some of the models show in their edge-on views a conspicuous b/p morphology, while their face-on views show clearly that they are non-barred, and even in some cases almost axisymmetric. It is clear that, at least in these cases, the b/p morphology is due to the internal dynamics of the self-consistent model and not to merging phenomena.

In this paper we will first describe a particularly illustrative simulation (Section 2). We then use orbital theory to understand the dynamics of b/p structures. We use a purely axisymmetric potential consisting of a disc and a halo component (Section 3), in order to identify the orbits that constitute the backbone of the b/p structure (Section 4). The edge-on profiles are discussed in Section 5. We discuss our results in Section 6, and we stress the fact that it is the existence of vertical resonances *per se* and not the kind of perturbation that gives rise to the appearance of b/p morphologies.

2 THE *N*-BODY MODEL

Athanassoula's *N*-body stellar model starts with initial conditions created by the method of Hernquist (1993) and consists of an exponential disc with a sech^2 vertical dependence, and a halo profile proposed by Hernquist (1993). The detailed description of the disc and halo initial density distributions can be found in Athanassoula & Misiriotis (2002, equations 1 and 3).

In computer units the mass of the disc is taken as $M_\mathrm{d} = 1$, the halo mass $M_\mathrm{h} = 5$, the disc scalelength $h = 1$, the scaleheight of the disc $z_0 = 0.2$ and the halo scalelength $\gamma = 5$. The rest of the parameters of the model in equations (1) and (3) of Athanassoula & Misiriotis (2002) are as described in section 2 of the above mentioned paper. In the simulation we present here we can assume the unit of mass to be $5 \times 10^{10}\,\mathrm{M}_\odot$, the length unit to be 3.5 kpc, the unit of velocity to be 248 km s^{-1} and the time unit to be 1.4×10^7 yr. The simulation has 200 000 particles in the disc and the halo is live and composed of 931 206 particles. The Toomre parameter Q is 1.8 (Toomre 1964). We underline the lack of an explicit bulge component. The simulation

⋆E-mail: ppatsis@cc.uoa.gr

was carried out on a Marseille Observatory GRAPE-5 system using a tree code similar to the one described by Athanassoula et al. (1998). For more details we again refer the reader to Athanassoula & Misiriotis (2002). A characteristic snapshot of the simulation after 8.4 Gyr from the start is given in Fig. 1. The upper panel gives the circular velocity curve, which is rising and reaches approximately 0.68 (i.e. ≈ 170 km s^{-1}) at 5 unit lengths (i.e. 17.5 kpc). The dashed and dotted lines give the disc and the halo contributions, respectively. The second, third and fourth panels from the top give the isodensities of the disc particles projected face-on, side-on and end-on respectively. The bottom panel gives the dot-plot of the particles in the (x, y) plane. The side of the box for the face-on views is 10 units (i.e. 35 kpc), so the height of the boxes for the edge-on views is 3.33 units (i.e. ≈ 11.65 kpc). From the face-on view it is evident that the model essentially does not have a bar. One can speak about a weak overall oval distortion. Such a weak perturbation can be detected in a large fraction of disc galaxies as an $m = 2$ component of low amplitude. Nevertheless, both side-on and end-on views are obviously boxy. The fact that the relative extent of the b/p feature is about the same when projected on the horizontal axes reflects the fact that the isocontours of the density in the face-on view are nearly round.

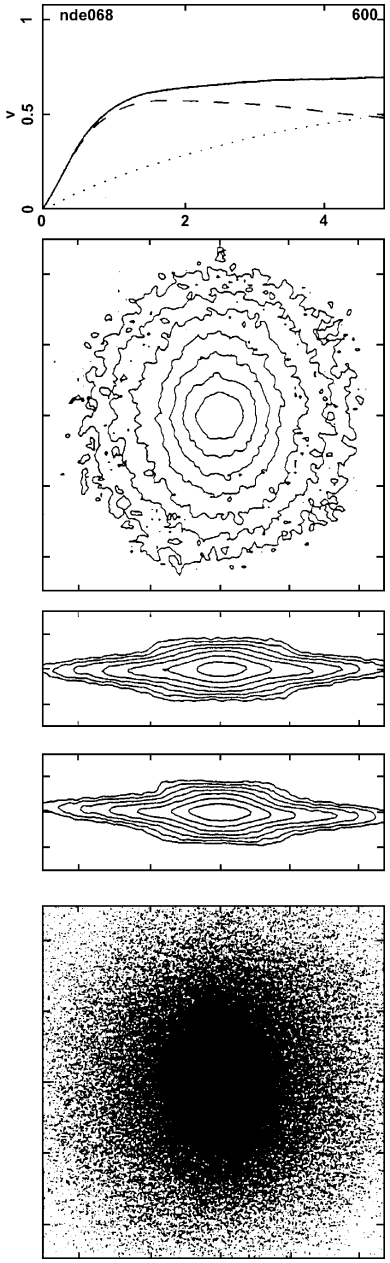

Figure 1. Basic information on the stellar *N*-body simulation. From top to bottom are depicted the circular velocity curve (the dashed line gives the disc and the dotted the halo contribution), the isodensities of the disc particles projected face-on, side-on and end-on, and finally the dot-plot of the particles in the (x, y) plane. The side of the box for the face-on views is 10 units, i.e. (with the adopted normalization) 35 kpc, and the height of the boxes for the edge-on views is 3.33 units, i.e. ≈ 11.65 kpc. In the top panel we give the name of the model and the time at which the snapshot was taken.

3 THE ORBITAL MODEL

For our orbital calculations we will use a general axisymmetric potential consisting of a disc and a halo component. We adopt a Miyamoto & Nagai (1975) disc potential, $\Phi_{\rm D}$, which in cylindrical coordinates has the form

$$\Phi_{\rm D}(r, z) = -\frac{GM_{\rm D}}{\sqrt{r^2 + (a + \sqrt{z^2 + b^2})^2}}. \quad (1)$$

In the above the parameter $M_{\rm D}$ refers to the disc mass, a and b are the horizontal and vertical scalelengths respectively, and r and z are the cylindrical coordinates. The halo potential, $\Phi_{\rm H}$, is given by

$$\Phi_{\rm H}(r, z) = \frac{v_{\rm H}^2}{2} \ln\left[1 + \frac{1}{r_{\rm c}^2}(r^2 + z^2)\right], \quad (2)$$

where $v_{\rm H}$ is the limiting circular velocity as $r \to \infty$, and $r_{\rm c}$ is the core radius of the halo. The total potential used for the orbital calculations is of the form $\Phi = \Phi_{\rm D} + \Phi_{\rm H}$, and the adopted values of the parameters are $M_{\rm D} = 6 \times 10^{10}\,{\rm M}_{\odot}$, $a = 3$ kpc, $b = 1.5$ kpc, $r_{\rm c} = 18$ kpc and $v_{\rm H} = 176.8$ km s^{-1}. The rotation curve (Fig. 2) reproduces fairly well that of the *N*-body model presented in the previous section. One can clearly see that we have a model with a maximum disc, as in the case of the *N*-body model. We remind the reader that

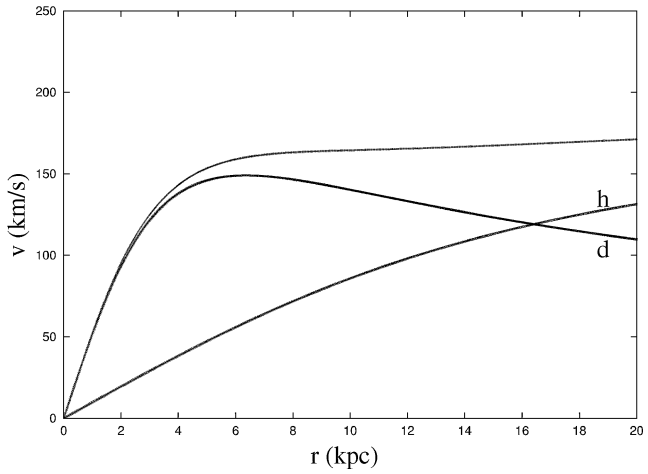

Figure 2. The rotation curve for the orbital model. It shows that the mass distributions in the *N*-body and the orbital model are very close. The disc contribution is indicated with a 'd' and that of the halo with an 'h'.

5 length units in the *N*-body model correspond to 17.5 kpc, and its velocity unit is 248 km s^{-1}.

4 ORBITS AND ORBITAL BEHAVIOUR

The calculations have been done in Cartesian coordinates in a frame of reference rotating around the z-axis. Thus the Hamiltonian governing the motion of the test particles is

$$H = 1/2(\dot{x}^2 + \dot{y}^2 + \dot{z}^2) + \Phi(x, y, z) - 1/2\Omega_p^2(x^2 + y^2), \qquad (3)$$

where Ω_p is the pattern speed. In the following we will denote by E_j the numerical value of H and adopt for the pattern speed the value $\Omega_p = 11.9$ km s^{-1} kpc^{-1}, which places corotation approximately at 14 kpc.

On the equatorial plane we can define the radial resonances between the epicyclic frequency and the angular velocity in the rotating frame. In a 3D model we can also define vertical resonances, which involve the vertical instead of the epicyclic frequency (for definitions see e.g. Binney & Tremaine 1987). The first vertical resonance in our model is the 3 : 1.

The main family in our model is the family of direct circular periodic orbits on the $z = 0$ plane. These orbits, in the presence of a spiral or barred perturbation, become ellipses, the well known x1 orbits (see e.g. Contopoulos & Grosbøl 1986, 1989). By analogy, we will call this family x1 also in our axisymmetric model. In 2D models the orbits of this family support the spiral or bar structure. The stability of a periodic orbit is characterized by the behaviour of two indices b_1 and b_2. In this study, the stability index b_1 is associated with the motion perpendicular to the equatorial plane, while b_2 is associated with radial perturbations. A family is stable if both stability indices b_i are $-2 < b_i < 2$ (Hadjidemetriou 1975). For more details on the stability of families of periodic orbits in 3D systems, the reader should refer to Contopoulos & Magnenat (1985).

The most important families of periodic orbits for the dynamics of a 3D disc galaxy are the central family and those bifurcated from it at the vertical $n : 1$ resonances, where n is a small integer. At these resonances, in the axisymmetric case, index b_1 of family x1 becomes tangent to the $b = -2$ axis. The bifurcated families come actually in pairs[1] and are in this case marginally stable because they always have one of their stability indices on the $b = -2$ axis, while the other remains always between -2 and *2*. The variations of the stability indices b_1 and b_2 of the x1 family, as well as those of the families bifurcated at the vertical resonances 3 : 1, 4 : 1, 5 : 1, 6 : 1 and 7 : 1, are given in Fig. 3 as a function of the Jacobian E_j. The vertical black arrows indicate the points where index b_1 of x1 becomes tangent to the $b = -2$ axis at the vertical resonances. Horizontal arrows point to the index of each bifurcating family which oscillates between -2 and 2. They are always given close to the value of the Hamiltonian at which the family bifurcates from the x1. The introduction of a barred or spiral perturbation in the model brings into the system a stable and an unstable family. For the stable one the index which in the axisymmetric case was lying on the $b = -2$ axis now becomes absolutely smaller than 2, so the family remains stable over a large radial region (Patsis & Grosbøl 1996; Skokos, Patsis & Athanassoula 2002a,b). The vertical white arrows indicate the tangencies of the index b_2 of the x1 family with the $b = -2$ axis at the radial resonances.

[1] The two families, which bifurcate at a tangency of a stability index with the -2 axis in the axisymmetric case, have a stable and an unstable counterpart in the non-axisymmetric case.

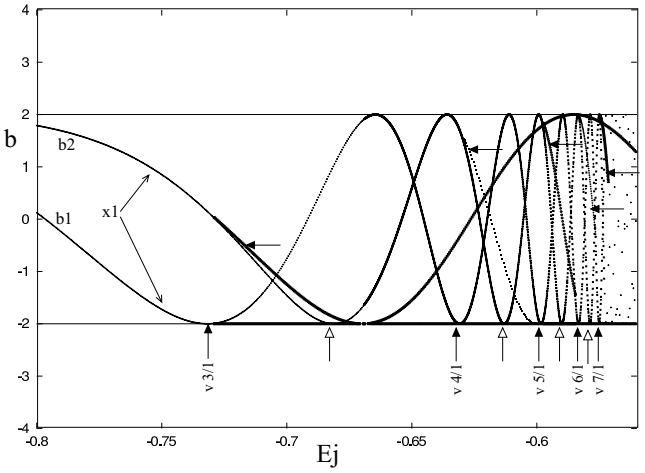

Figure 3. The stability indices b_1 and b_2 of the central family x1 as a function of E_j, where E_j is the value of the Hamiltonian. We give also the stability indices of the families bifurcated at the vertical resonances 3 : 1, 4 : 1, 5 : 1, 6 : 1 and 7 : 1. One of their stability indices remains always equal to 2, while the other one oscillates between -2 and 2.

5 THE EDGE-ON PROFILE

Most stars in a galaxy will move along non-periodic orbits trapped around stable periodic orbits (Poincaré 1992). Thus the topology of the main families of periodic orbits will determine the basic features in the galaxy. In the present case the main families are the central family and the families bifurcated at the vertical resonances, which exist as two branches symmetric with respect to the equatorial ($z = 0$) plane. The response density profile is a weighted average of the individual orbit contributions. As a weight, we use the disc density, $\rho_D(r, z)$, where ρ_D is the density corresponding to the Miyamoto disc calculated at the position (r, z), where r is the radius of the circular equatorial plane orbit which has the same E_j as the orbit to be weighted and z is the mean vertical distance of the orbit from the equatorial plane. We have adopted the density of the luminous (disc) component because the orbital profiles will have to reproduce the light distribution, when we compare with real galaxies, or the disc component of the *N*-body simulations.

Since our model is axisymmetric we can use arbitrarily any two orthogonal axes on the equatorial plane in order to calculate periodic orbits. This means that a periodic orbit rotated around the axis of symmetry (z-axis) is also a periodic orbit of the system. The projections of these periodic orbits on a given axis will always be confined within certain limits determined by a maximum length and a maximum height. We also note that the orbits of the two families that bifurcate from the central family at the tangencies of the b_1 index with the $b = -2$ axis (Fig. 3), at a given E_j value, are topologically similar.

We have calculated at each energy (E_j) only one periodic orbit per family along our x-axis. We started with the orbit that has the same radius as the circular orbit at the E_j where the family is bifurcated, and we followed the evolution of the family by finding the orbits along the specific x-axis. These orbits have been used for constructing the profiles in Fig. 4. Nevertheless, at each energy, one can find, by rotation, an infinite number of representatives of the same family, owing to the axisymmetric nature of the potential. It is the same as viewing a given orbit from all possible viewing angles by rotating our point of view around the z-axis, while staying always on the equatorial plane.

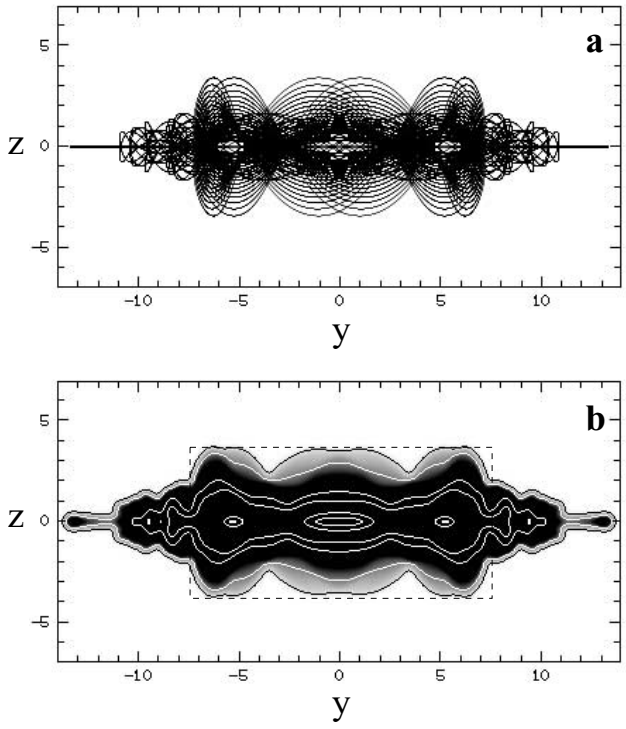

Figure 4. The (y, z) orbital profile: (a) the profile of the weighted orbits; (b) the corresponding blurred image. The dashed box indicates the area that is filled if all orbits at a given energy are considered.

In the (y, z) profile, created by (marginally) stable orbits of the families considered in Fig. 3 (Fig. 4a), we observe a 'stair-type' structure with a central boxy region. This central region is formed by the orbits of the two branches (symmetric with respect to the equatorial plane) of the 3D family bifurcated at the vertical 3 : 1 resonance. By applying a smoothing filter to the image with the weighted orbits we obtain a blurred profile, which, to a first approximation, can be considered as the profile for the density distribution of the model. This blurred profile is shown in Fig. 4(b). By considering all possible orbits at each energy, the area inside the rectangle drawn with a dashed line in Fig. 4(b) will be filled. The (x, z) profile, when considering all orbits, will be identical to the (y, z) one, as expected. In Fig. 4(b) we illustrate the resulting morphology by using isocontours. Clearly the profiles of the orbital model (Fig. 4) and the profiles of the *N*-body simulation (Fig. 1) have many similarities. First of all we have a boxy structure confined within radii less than 2 length units of the *N*-body simulation, which correspond to 7 kpc. This is practically the radius in Fig. 4 inside which we find the boxy structure of the orbital model. Also the 'stair-type' edge-on profiles of the weighted orbits are in good agreement with the outer parts of the edge-on profiles of the *N*-body model.

6 DISCUSSION

In the present study we propose a mechanism which can account for boxy structures in the edge-on profiles of non-barred disc galaxies. In the example that we present here, it is the presence of the vertical 3 : 1 resonance that introduces this structure into the system. It is, however, not necessary to have a particular vertical resonance in order to form a b/p profile. Furthermore, since radial and vertical resonances can be defined even in an axisymmetric case, one can find even in the axisymmetric model the bifurcating orbits that give rise to these features. In fact, the only two necessary ingredients are

(i) the presence of a vertical n : 1 resonance, where n is a small integer, so that a new family, bifurcating at this point, is introduced in the system, and

(ii) that the bifurcated family should be stable over a sufficiently large E_j interval and should trap a sufficient number of regular orbits around it.

If these two conditions are fulfilled, the 'stair-type' orbital profile follows naturally, because the successive 3D families lower their mean heights as the energy at which they are bifurcated from x1 increases. In addition, as energy increases, the successive orbits of a bifurcating 3D family increase their mean spherical radius by growing more in z than in their cylindrical radius and, beyond a critical energy, by growing practically only in the vertical direction. Since their cylindrical radius – or extent along the equatorial plane – is thus limited, while their vertical extent is large, at least for large values of the Jacobi energy E_J, they contribute to a boxy profile. As we have shown here, it is not necessary to have a strong perturbation in order for the vertical extent to be important. Thus the boxy feature can be strong and clearly defined, even in a purely axisymmetric model.

If we introduce a perturbation, the topology of the relevant orbital families remains the same and they will be stable rather than marginally stable (Patsis & Grosbøl 1996; Skokos et al. 2002a,b). There will, however, be one morphological difference, owing to the fact that in the non-axisymmetric case the rotational symmetry is broken. In this case it will not be possible to have orbits of any desired azimuthal orientation, and as a result we will have a 'peanut-shaped' profile, at least for a range of viewing angles, instead of a boxy one.

Lack of a boxy structure in a model indicates one of the following three possibilities: vertical resonances with small n : 1 do not exist in the system; or the family bifurcated at the vertical resonance with the lowest E_j value has unstable parts that are too large; or, for reasons that could be linked to the formation history of the galaxy, too few stars are on orbits trapped around the stable periodic n : 1 orbits. The conditions needed for building a b/p profile may be favoured by the presence of the bar, but the bar *per se* is not the reason that edge-on disc galaxies have boxy profiles. Of course our mechanism relies on the existence of a pattern speed that does not vary much with time. In other words it implicitly assumes the existence, or past existence, of some non-axisymmetric feature, albeit of perhaps infinitesimal amplitude.

Bureau & Freeman (1999) and Athanassoula & Bureau (1999) developed diagnostics to detect the presence and orientation of a bar in edge-on disc galaxies. They detected in most of the peanut-shaped edge-on galaxies in Bureau & Freeman (1999) the signature of a 'x2-flow' in the position–velocity diagrams. This was taken as the manifestation of the presence of a bar. However, in a few cases, this feature was absent. Athanassoula & Bureau attributed the lack of such a feature either to a lack of an inner Lindblad resonance (ILR) or to a lack of emitting gas around the ILR region. The present study adds a third possibility, namely that the galaxy is not barred.

ACKNOWLEDGMENTS

We acknowledge fruitful discussions with and very useful comments by Professor G. Contopoulos. We also thank the anonymous referee for comments which improved the paper. This work has been supported by the Research Committee of the Academy of Athens. EA

also thanks the IGRAP, the Region PACA, the INSU/CNRS and the University of Aix-Marseille I for funds to develop the GRAPE computing facilities used for the simulations discussed in this paper. PAP and ChS thank the Laboratoire d'Astrophysique de Marseille, for an invitation. ChS was supported by the 'Karatheodory' fellowship No. 2794 of the University of Patras.

REFERENCES

Athanassoula E., Bureau M., 1999, ApJ, 522, 699
Athanassoula E., Misiriotis A., 2002, MNRAS, 330, 35
Athanassoula E., Bosma A., Lambert J.-C., Makino J., 1998, MNRAS, 293, 369
Binney J., Tremaine S., 1987, Galactic Dynamics. Princeton Univ. Press, Princeton, NJ
Bureau M., Athanassoula E., 1999, ApJ, 522, 686
Bureau M., Freeman K. C., 1999, AJ, 118, 126
Combes F., Sanders R. H., 1981, A&A, 96, 164
Combes F., Debbasch F., Friedli D., Pfenniger D., 1990, A&A, 233, 82
Contopoulos G., Grosbøl P., 1986, A&A, 155, 11
Contopoulos G., Grosbøl P., 1989, A&AR, 1, 261
Contopoulos G., Magnenat P., 1985, Celest. Mech., 37, 387
Hadjidemetriou J., 1975, Celest. Mech., 12, 255
Hernquist L., 1993, ApJS, 86, 389
Kuijken K., Merrifield M. R., 1995, ApJ, 443, L13
Lütticke R., Dettmar R.-J., Pohlen M., 2000, A&AS, 145, 405
Miyamoto M., Nagai R., 1975, PASJ, 27, 533
Patsis P. A., Grosbøl P., 1996, A&A, 315, 371
Pfenniger D., 1984, A&A, 134, 373
Pfenniger D., 1985, A&A, 150, 112
Pfenniger D., Friedli D., 1991, A&A, 252, 75
Poincaré H., 1892, Les méthodes nouvelles de la mécanique céleste. Gauthier-Villars, Paris
Raha N., Sellwood J. A., James R. A., Kahn F. D., 1991, Nat, 352, 411
Skokos Ch., Patsis P. A., Athanassoula E., 2002a, MNRAS, 333, 847
Skokos Ch., Patsis P. A., Athanassoula E., 2002b, MNRAS, 333, 861
Toomre A., 1964, ApJ, 139, 1217

This paper has been typeset from a TEX/LATEX file prepared by the author.